Probing the SEB Sensitive Depth of a Power MOSFET Using a Two-Photon Absorption Laser Method

Jean-Marie Lauenstein, *Member, IEEE*, Sandra Liu, *Member, IEEE*, Jeffrey L. Titus, *Senior Member, IEEE*, Dale McMorrow, *Member, IEEE*, Megan C. Casey, *IEEE Member*, Stephen P. Buchner, *IEEE Member*, Jeffrey Warner, Anthony M. Phan, Alyson D. Topper, Hak S. Kim, Kenneth A. LaBel, *IEEE Member*, Becky Yang, Max Zafrani, and Phillip Sherman

***Abstract*—This paper presents two-photon absorption test results on an engineering single-event burnout- (SEB-) sensitive power MOSFET to verify that the energy deposition/charge ionization in the highly-doped substrate does not contribute to SEB. It is shown that for a vertical power MOSFET, the SEB sensitive volume is the lightly doped epitaxial layer; the most sensitive region is under the polysilicon gate.**

***Index Terms*— power MOSFET, single-event burnout (SEB), two-photon absorption**

I. Introduction

A growing body of studies have sought to characterize the single-event burnout (SEB) sensitive volume in vertical power MOSFETs [1-7]. These studies include both single-photon absorption laser and heavy ion irradiations from the frontside and backside of the device. Despite these efforts, confusion remains regarding the sensitive depth for triggering SEB – particularly the role of charge ionized in the highly-doped drain substrate region. Accurate determination of the SEB sensitive depth is important for guiding radiation hardness assurance methods. Many heavy-ion accelerator test facilities lack the high energy ions required for penetration deep into the substrate region of high-voltage power MOSFETs.

The goal of this work is to identify the SEB sensitive depth with high resolution in order to determine if the energy deposition in the highly doped substrate plays a role in the SEB failures. In order to eliminate the complication of a trail of energy deposition (ionized charge along an ion track or a long single-photon laser path), the two-photon absorption (TPA) laser method was chosen. This method is also capable of focusing energy anywhere in the silicon with a very small laser spot size (micro beam). TPA provides the possibility to evaluate the SEB sensitive depth with 5 – 10 um accuracy in a power DMOSFET structure.

II. Sample Preparation

An SEB-sensitive engineering device was fabricated for this study by modifying the process of an existing International Rectifier product, the IRHC57230SE. Most commercial and older-generation radiation hardened power MOSFETs are sensitive to both SEB and single-event gate rupture (SEGR), and are thus not good candidates for SEB studies due to the interference from SEGR failures. Newer generation radiation hardened power MOSFETs are typically SEB and SEGR hardened, and therefore are not good candidates for SEB studies either.

In addition to making an SEB-sensitive device, there were also multiple challenges in preparing a power DMOSFET for TPA analyses. Integrated circuits (ICs) have multiple layers of metal on the chip surface, but do not have metal on the backside of the chip. It is therefore possible to thin the backside of the chip to make the devices suitable for laser experiments. For power DMOSFETs, the backside of the die is used as the drain contact. To reduce drain contact resistance, a multilayer metal film is deposited at the backside. To prepare samples for this study, a special engineering device was fabricated without this regular backside metal. This engineering die was then thinned to about 85 μm in total

Manuscript received July 22, 2011. This work was supported in part by International Rectifier Corporation, the NASA Electronic Parts and Packaging Program (NEPP), and the Defense Threat Reduction Agency (DTRA) under IACRO# 10-4977I, IACRO# 11-4395I.

J.-M. Lauenstein, M. C. Casey, and K.A. LaBel are with NASA/GSFC, Code 561.4, Greenbelt, MD 20771 (USA), email: jean.m.lauenstein@nasa.gov, megan.c.casey@nasa.gov, and kenneth.a.label@nasa.gov.

S. Liu, B. Yang, M. Zafrani, and P. Sherman are with International Rectifier Corporation,

A. M. Phan, A. D. Topper, and H. S. Kim are with MEI Technologies, Inc., work performed for NASA/GSFC, Code 561.4, Greenbelt, MD 20771 (USA), email: anthony.m.phan@nasa.gov, alyson.d.topper@nasa.gov, and hak.s.kim@nasa.gov.

F. A. Author is with the National Institute of Standards and Technology, Boulder, CO 80305 USA (corresponding author to provide phone: 303-555-5555; fax: 303-555-5555; e-mail: author@ boulder.nist.gov).

S. B. Author, Jr., was with Rice University, Houston, TX 77005 USA. He is now with the Department of Physics, Colorado State University, Fort Collins, CO 80523 USA (e-mail: author@lamar.colostate.edu).

T. C. Author is with the Electrical Engineering Department, University of Colorado, Boulder, CO 80309 USA, on leave from the National Research Institute for Metals, Tsukuba, Japan (e-mail: author@nrim.go.jp).

To be presented by Sandra Liu at the International Electrical and Electronics Engineering (IEEE) Nuclear and Space Radiation Effects Conference (NSREC), July 26, 2011, Las Vegas, NV., and published on nepp.nasa.gov and radhome.gsfc.nasa.gov.

thickness because the intensity of the TPA laser decreases as it passes through highly-doped silicon material. With ~7 μm non-silicon materials on the die surface and a ~20 μm epitaxial silicon layer, this engineering die has less than 60 μm of highly doped silicon substrate. The smoothness of the backside silicon surface is important as well: if the surface is rough, laser intensity will be reduced due to surface reflections. In order to ensure smoothness, the backside of the die surface (the highly doped substrate) was polished at the wafer level.

The die were specially assembled to provide access to the backside. Conductive silver epoxy was used for the die attach process and a hole was drilled in the package to allow laser access. The silver epoxy was only applied to both ends of the die, rather than covering the whole backside as in a regular assembly. Fig. 1 shows an assembled sample used for TPA analyses.

Some samples were also assembled in regular TO-3 package using silver epoxy for front side heavy ion tests, in addition to heavy ion tests from the backside. These data were used as a guide in determining the appropriate drain bias for the TPA experiments.

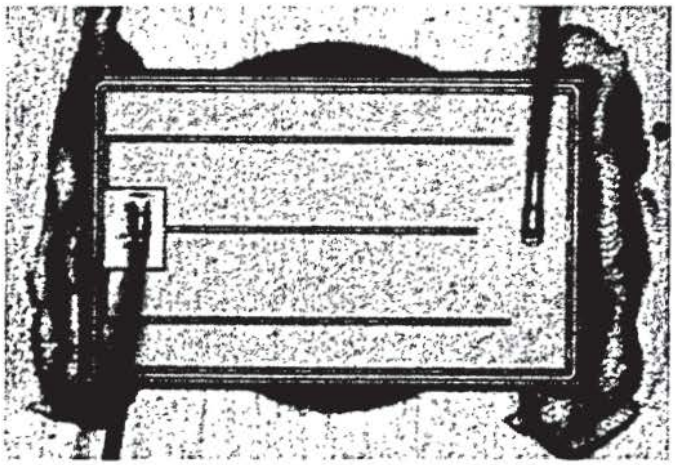

Fig. 1. Top view of an engineering 57230SE sample built for backside TPA studies. A hole drilled in the packaging allows laser access to the polished backside of the device.

III. Test Setup & Procedure

The TPA experimental setup (Fig. 2) is similar to that used in heavy-ion (broad beam) tests. A special bias board was designed and built to facilitate the TPA test. The small network attached between the gate power supply (Vgs SMA input) and the device's gate node is a balanced low-pass filter to prevent switching spikes and other anomalies from causing gate damage. A Tektronix CT-2 probe is inserted in series with the drain, and is connected (IPP SMA Output) to a Tektronix

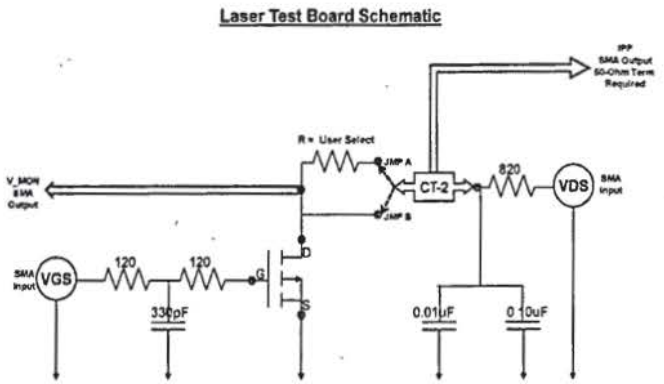

Fig. 2. Bias board schematic for the TPA laser tests.

TDS5104B oscilloscope allowing beam-induced transients to be captured. The oscilloscope is adjusted to trigger on each laser pulse. A current-limiting resistor can be placed optionally in series with the drain in front of the probe. Two stiffening capacitors provide current to the device, preventing the drain voltage from sagging due to power supply limitations. Two current-voltage sourcing and measurement instruments (SMUs) were used for testing: a Keithley 2400 for the gate bias and a Keithley 2410 for the drain bias.

The bias board is mounted to an x-y-z optical stage having 10 nm x-y resolution and 500 nm resolution in the z-direction. Moving the stage in the z-direction allows the beam to be focused to different depths within the device. The laser was focused through a 100X objective. Fig. 3 shows the test board mounted to the stage, with the device under test (DUT) positioned in the path of the focused laser.

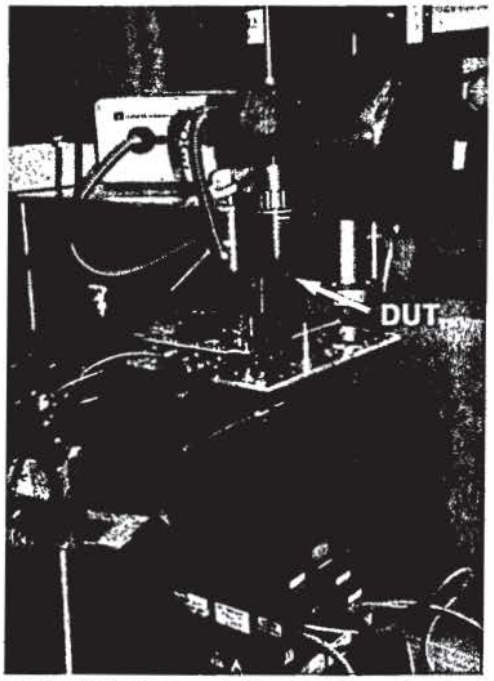

Fig. 3. Sample (DUT) mounted on test board atop the fully-mechanized stage. Laser is focused through the 100X objective above the sample.

To be presented by Sandra Liu at the International Electrical and Electronics Engineering (IEEE) Nuclear and Space Radiation Effects Conference (NSREC), July 26, 2011, Las Vegas, NV., and published on nepp.nasa.gov and radhome.gsfc.nasa.gov.

The laser system is well-described in [8]. Its wavelength is 1260 nm and pulses in silicon at a 1 kHz frequency with a 100 fs pulse width. The focused (1/e contour) spot size has a 1.35 μm waist and about a 10 μm depth within the silicon. Fig. 4 depicts the laser energy as a function of distance from the focal waist. Note that the charge density is proportional to the square of the intensity of the laser beam, but because intensity is proportional to $1/r^2$ (where r is the radial distance from the long axis of the ellipsoidal focal area), the ionized charge density falls off as $1/r^4$.

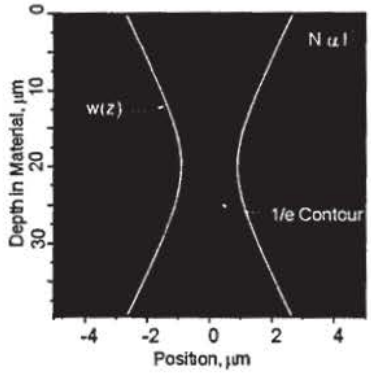

Fig. 4. Contour of TPA laser intensity showing the 1/e contour defining the focal area. Charge ionization falls off as $1/r^4$ where r is the distance along the x-axis away from the center of the focal area.

The test procedure is briefly summarized here. Different regions within the MOSFET cell were selected for SEB sensitivity studies. The actual device thickness was verified by first focusing the laser on the backside of the device (substrate surface), then moving into the device until the cell topology came into focus (see Fig. 4A), which was at the device silicon surface. The distance traveled in the z-direction confirmed the device thickness is around 85 μm as processed. Fig. 5A is a typical picture when viewed from the backside with focus at the device surface (gate and source side). The lighter stripes are the locations of polysilicon gates, while the darker lines indicate source contacts. For SEB sensitivity comparisons, the laser beam is focused at various locations for each scan. Fig. 5B shows the typical path of the laser scanning path for this TPA SEB study. The Naval Research Laboratory's Single Event Effects 3D Mapping program (SEE3D) controls the micro stage and is set to have the laser scan through the entire highly doped substrate, move into the lightly doped epitaxial region, and out of the non-silicon surface layers. The scan step size is set at 1.75 μm; all depths are measured from the backside surface of the die.

At each step, 25 laser pulses were delivered. As can be seen in Fig. 6 inset, non-overlapping drain current transients resulted from these pulses. The energy of the laser fluctuates minimally; to minimize energy fluctuation effects on the SEB sensitivity mapping, the resulting 25 transients from the laser pulses were averaged. The drain and gate biases (Vds and Vgs, respectively) are set to desired values before the laser scan starts. Both protective mode (external drain load resistor added

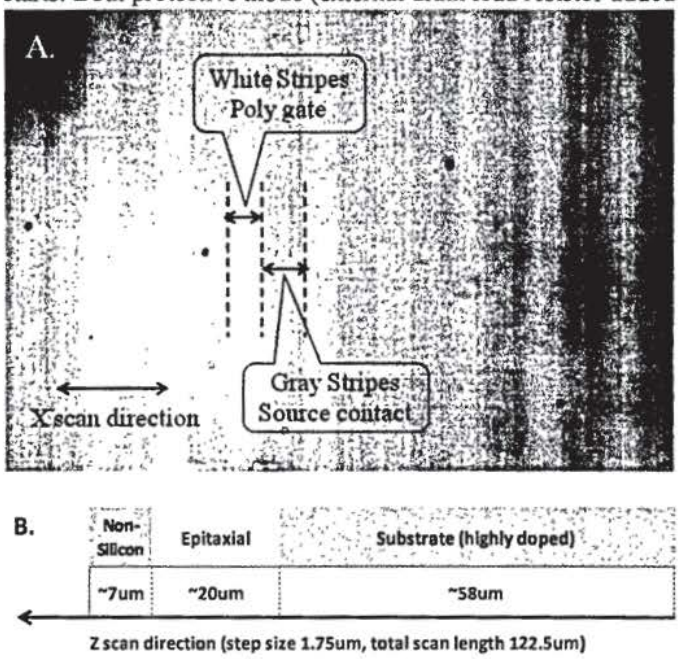

Fig. 5A. Picture showing white and dark lines as seen from the backside of the sample. Lighter stripes correspond to polysilicon gate lines, darker lines indicate the region beneath the source contacts. B. Illustration of the different layer thicknesses within the DUT. All scans began at the back surface of the sample; scan directions are indicated in the figure.

at the drain contact) and unprotected mode (no external drain resistor) laser irradiations were performed. The load resistor allowed protective SEB sensitivity evaluation under various biases, laser energies, and in the different active cell locations. The unprotected mode was used to confirm the SEB sensitivity.

Prior to this study, engineering 57230SE samples built in the normal assembly scheme were tested with various heavy ions at the Texas A&M University (TAMU) cyclotron facility. Test results show this device is sensitive to SEB, with the threshold at about 85 V drain bias when tested with xenon under both destructive and protective modes. For these TPA SEB sensitivity studies, a 100-volt bias is therefore applied to the drain to ensure SEB will be triggered, and a 1-kΩ resistor is used to provide needed protection from destructive SEB failure. Finally, each sample was electrically characterized prior to use and following each run performed in unprotected mode.

IV. Test Results and Analyses

A. SEB Sensitivity as a Function of Active Cell Topology

For initial TPA studies, the laser beam was focused at various locations along the active cell and then allowed to scan from the backside of the substrate toward the device surface. The beam energy was adjusted to 7.41 nJ and the device was

biased at 0 Vgs and 100 Vds. A 1 kΩ resistor at the drain contact protected the device from damage. Fig. 6 shows typical examples of observed transient curves measured when the laser positioned in the middle of epitaxial thickness (a depth of 70 μm), for 4 different locations within the active cell. These locations are: the center of the polysilicon gate (white stripe), the base region (on the boundary of the white and grey stripes), at the edge of the polysilicon gate (within the grey stripe at the edge of the white stripe), and beneath the source contact (center of the grey stripe). No transients were recorded in this latter location under these beam conditions. The transients in the other three regions are very similar in amplitude and width. At this voltage bias and beam energy, destructive SEB would occur in the absence of the external drain resistor.

The advantage of repeated laser pulses at a single location is the ability to capture whether an area is on the threshold of sensitivity. The inset in Fig. 6 provides a longer time scale revealing multiple transients in addition to the ones shown in the main plot. For the sake of clarity, only the transients recorded in the base region (as indicated by the red symbols) and at the edge of the poly gate (blue symbols) are shown. At 7.41 nJ laser energy, the less-sensitive edge of the poly gate does not register a drain transient with every laser pulse, whereas placing the focal area at the base region does. In this particular case, analysis of the transient data for the edge of the poly gate midway through the epilayer thickness reveals that

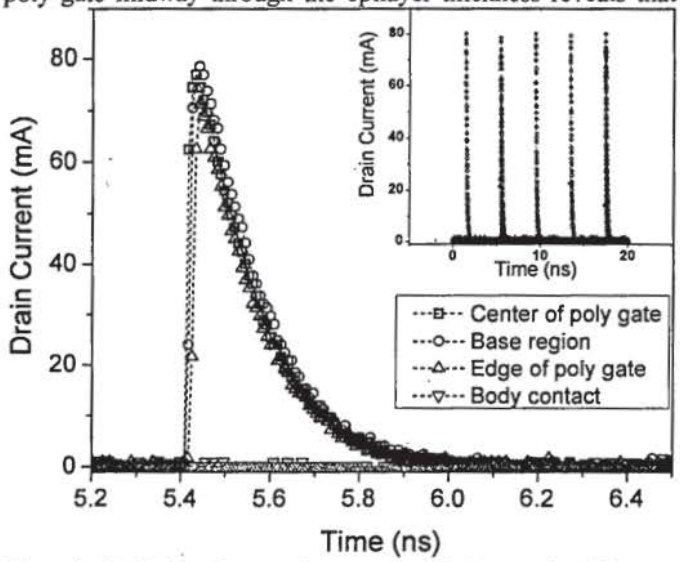

Fig. 6. Individual transients recorded at 4 different locations along the active cell at the center of the epilayer thickness. At 7.41 nJ, the laser could not induce SEB in the region under the body contact. Inset: On the boundary of the white and grey stripes (edge of the poly gate), SEB was triggered only occasionally, as shown in the inset.

only 5 large transients occurred during the 25 laser pulses at this location. A couple of very small (just above noise level) transients were also recorded. The large transients may be due to small fluctuations in the laser energy (± 10%), which may occasionally cross the energy threshold for this location. As indicated in section III above, the recorded transients for a given step are averaged; in this way, a location that undergoes SEB initiation with every laser pulse is differentiated from a location that only occasionally shows SEB vulnerability during the laser dwell time.

Examination of the transients plotted in Fig. 6 reveals that the area under the poly gate and the base region are more SEB-sensitive than the area at the edge of the poly gate and beneath the source contact. These data are a subset of the full scan through the depth of the device. In the next section, additional data are presented supporting this finding.

B. SEB Sensitivity as a Function of Laser Energy and Position in the MOSFET

As indicated in the previous section, for each given laser step, the average amplitude of the drain current transients was calculated. The SEB sensitivity was mapped in protective mode as a function of laser energy and depth within the device for the 4 different locations within the active cell. In Fig. 7A-7D, these sensitivity maps are shown. Six different laser energies were used: 5.56 nJ, 7.41 nJ, 9.27 nJ, 11.12 nJ, 12.97 nJ, and 14.82 nJ. These energies are indicated on the plots by the small black triangles along the y-axes.

The first apparent result is the dramatic absence of sensitivity except at very high energy in the region under the source contact (grey stripe), shown in Fig. 7D, as compared to under the polysilicon gate or base region (Figs. 7A and 7B, respectively). This finding is easily understood given the mechanisms of SEB. For an SEB event to be triggered, the parasitic bipolar junction transistor (BJT) formed by the source (emitter), body (base), and drain (collector) must be turned on. As ionized holes flow through the p-body region toward the source contact, the parasitic base-emitter junction becomes forward biased due to the resistance in the thin body region under the source. A positive feedback loop sets up from the gain of the BJT and additional charge generated by impact ionization as the electrons entering the depleted drain collector region are accelerated. If not limited, the high current levels will lead to secondary breakdown, permanently damaging the device.

The turn-on of the parasitic BJT is, therefore, key to initiating this SEB process. Charge ionized under the source contact results in the lowest current through the base, whereas holes ionized under the gate region that survive recombination must pass through this base to be collected. The elevated currents through the drain epitaxial region result in a shift in the peak electric field down to the epilayer/substrate interface [9, 10]. The field at the interface begins to grow when the parasitic BJT turns on, reaching its maximum at secondary breakdown. In these studies, protective mode testing prevents secondary breakdown, but the effect of the increased field at the epi/substrate interface can be seen in Figs. 7A and 7B. The interface lies close to 60 μm from the backside into these test devices. At this depth, there is a region of high-amplitude current transients.

In the base region (Fig. 7B), a second area of high-amplitude transients is found in the top 5-10 μm of the epilayer surface, corresponding to the base region. This area is where the electric field is initially at its peak.

When the laser focus is moved from under the gate, SEB becomes harder to trigger except with the higher laser energies, which has already been explained in terms of hole current density passing through the base region to be collected at the source contact. In Figs. 7A and 7B, the sensitive depth becomes narrower at the highest energies. This response may be an example of very high concentrations of ionized charge having a lower charge yield due to rapid recombination mechanisms that come into play.

From Fig. 7, it is clear that charge ionized in the highly-doped substrate does not result in drain current transients, in keeping with heavy-ion studies of SEB showing that the heavily-doped substrate region does not play a role in this failure mechanism [3, 4]. The high doping level will result in greater recombination of ionized charge. In addition, the electric field is not supported beyond the transition region; any charge surviving recombination will undergo slower diffusion transport.

Finally, transients occur after the focal area has moved into the initial few microns of the overlayers. This mapping is due to the ellipsoidal shape of the 1/e focal area, whose longitudinal axis extends about 5 μm above and below the focal waist (Fig. 4).

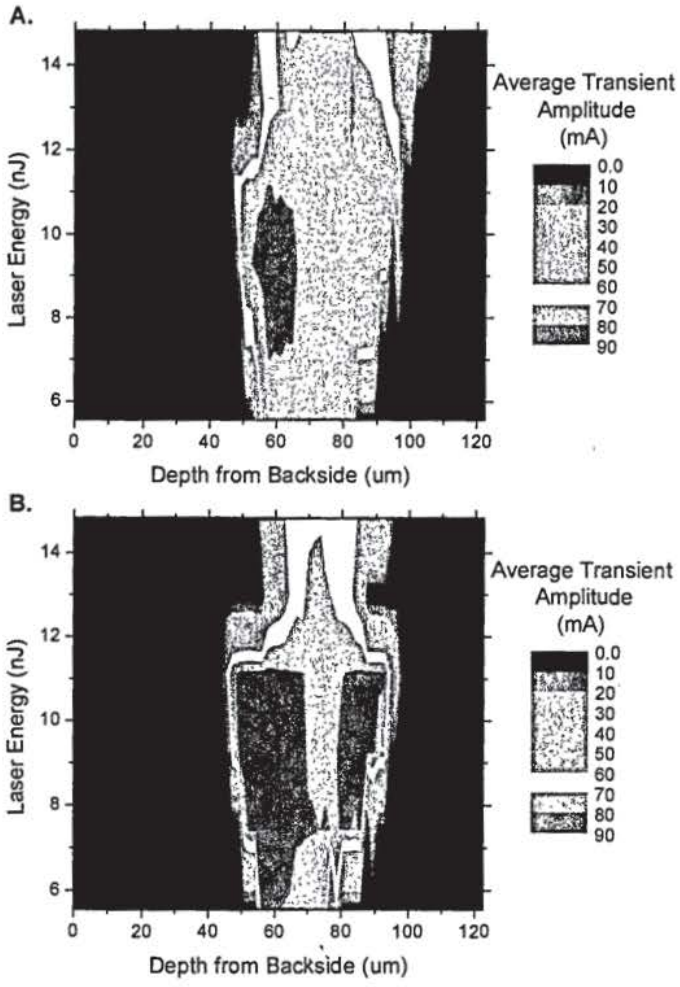

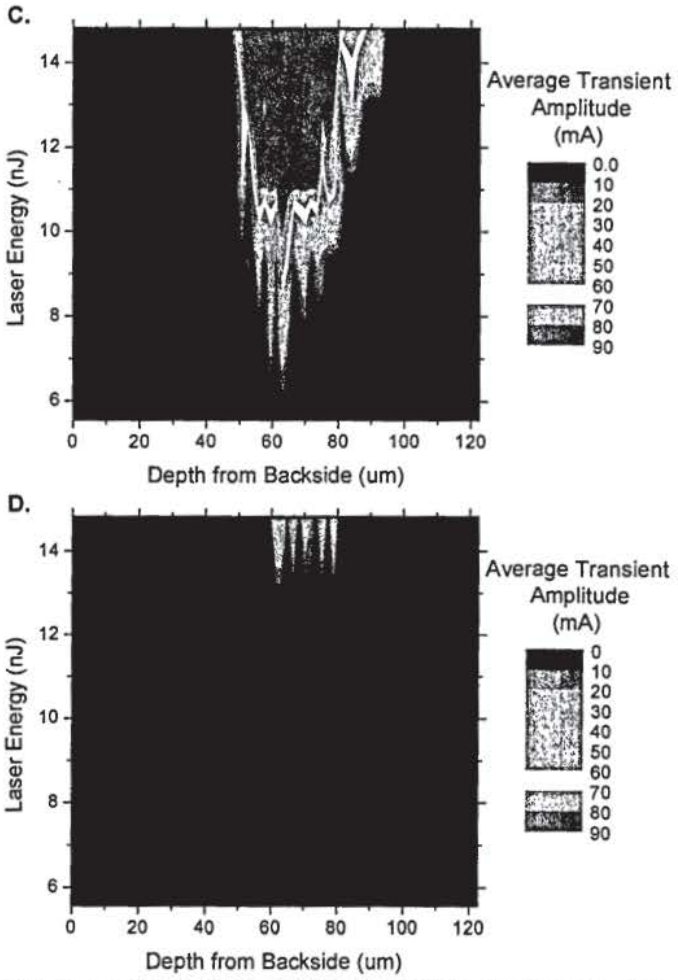

Fig. 7. Average drain current transient amplitude as a function of depth within the device (from the back surface) and of laser energy. Laser focus is at different x-axis locations, from under the gate to under the source contact: A. Beneath the center of the white stripe (poly gate); B. straddling the grey and white stripes (under the channel region); C. in the grey stripe at the edge of the white stripe (under the source diffusion); and D. under the center of the grey stripe (source contact). Drain bias 100 V; 1 kΩ load resistance.

C. Charge Ionization as a Function of Laser Energy

Fig. 8 compares the average amplitude of the transient signals at each scan step for different laser energies. When the laser energy increases, the area upon which the laser can focus and still induce SEB increases. At the lowest energy shown, the sensitive depth coincides with the epilayer thickness when the 5 μm axial radius of the focal area is accounted for (see Fig. 3). The charge density increases as the square of the energy increase, so even though a portion of the 1/e ellipsoid of high energy moves into the overlayers where the energy can no longer be absorbed, enough of the high-energy contour may remain in the epilayer region where it can still induce SEB. This would also be true as the focal area passes from the highly-doped substrate region into the epilayer: for a higher

laser energy, SEB will be triggered at a shallower depth (closer to the back surface of the die).

D. SEB Validation Through Destructive Mode Testing

Several samples were irradiated with the laser in an unprotected mode – that is, without the external drain resistor. Samples were biased at 100 Vds and 0 Vgs as before, and the laser energy set to the lowest value used in these studies (5.56 nJ). Fig. 9A shows the transient amplitude as a function of the scan depth under the center of the poly gate. The transients suddenly cease due to SEB. Fig. 9B shows the strip tape recordings from the SMUs where the drain current jumps high and remains high until power is removed.

E. SEB Validation with SEB-Hardened Device Analog

As indicated in section II, the above SEB tests were performed on a modified version of the IRHC57230SE, so that it would be susceptible to SEB within its rated bias level. Samples of the unmodified version (57260SE) were prepared for backside TPA tests in the same manner as for the modified die. These samples, which are known not to undergo SEB with heavy-ion testing, were tested using the same test setup and bias board. The laser energy was set at 7.41 nJ initially, and the device was scanned in the z-direction under the center of the poly gate. After each scan, the device electrically characterized to verify functionality. The drain bias was incremented between scans until the full 200 V bias was reached. The gate bias was then decremented in steps from 0 V down past the -20 V rating to -30 V. No destructive events occurred. Under the 200 Vds and -30 Vgs bias, scans were performed with the laser energy incremented to 14.82 nJ, and then finally to 18.53 nJ, whereupon the device failed. Based on these test results and understanding the process modification made for the engineering sample used in the SEB tests, the failures and protected mode high-current transients are due to SEB.

V. Failure Analysis

Some of the die that were tested in the unprotected mode later underwent failure analysis. Fig. 10 shows an image of the failure location (large dark star pattern) as seen from the back side of the sample through the 100X laser focusing objective. In Fig. 11, a SEM cross-section image reveals a typical burnout site due to TPA laser ablation.

VI. Summary

Engineering samples that were designed to be SEB sensitive were thinned to a total thickness of ~85 μm, without back metal. The die were attached with conductive silver epoxy to packages with access windows. These samples were then tested using a two-photon absorption method for evaluation of the SEB sensitive depth. The laser beam was focused at different depths starting from the highly-doped substrate and moving in steps to the lightly-doped epitaxial layer, under 4 different active cell regions. Results show the most sensitive region for SEB is in the base region. The charge ionized with the laser in the highly doped substrate did not contribute to the SEB failure mechanism.

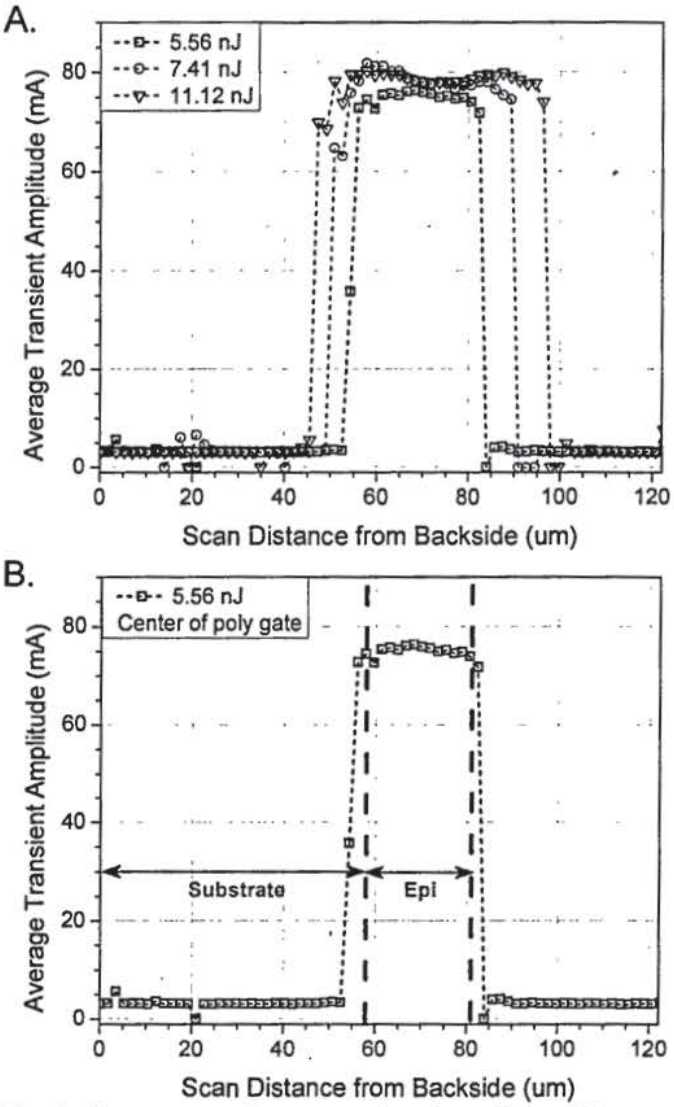

Fig. 8. Current transients as a function of scan distance into the DUT beneath the poly gate. A: As the laser energy increases, the sensitive depth appears to grow into the overlayers and substrate due to the enlarged energy contour of minimum ionized charge necessary to induce SEB. B: At the lowest energy, the sensitive depth coincides with the drain epilayer. Drain bias 100 V; 1 kΩ load resistance.

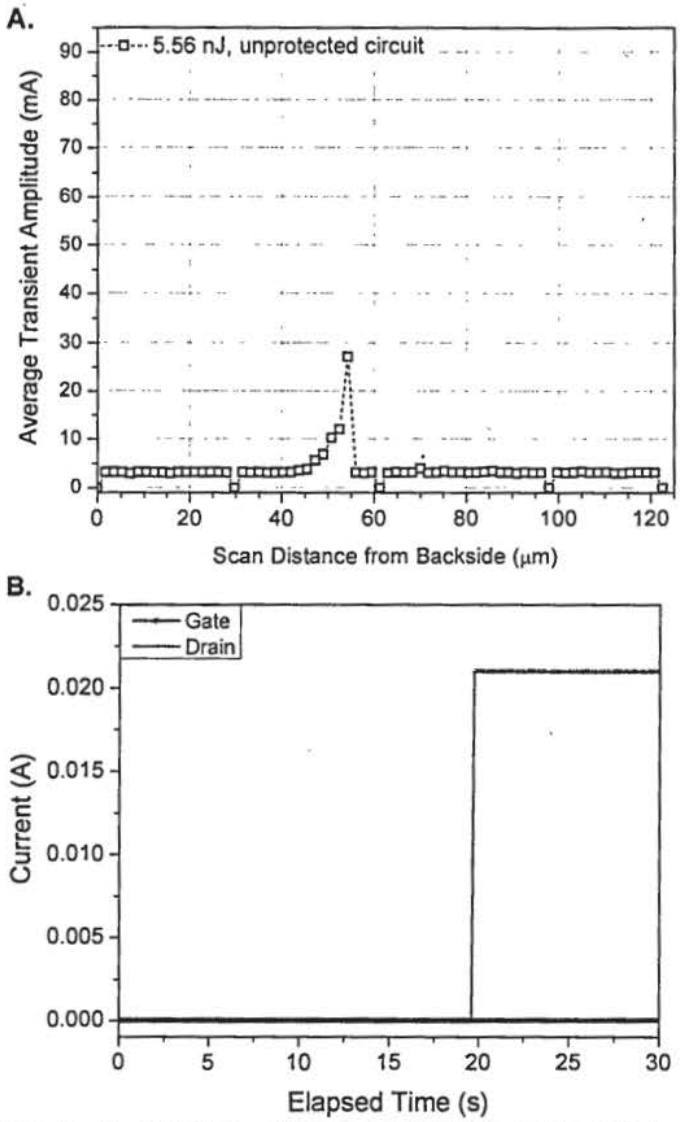

Fig. 9. A: Example of the scan results performed in unprotected mode (no external drain resistor) with the laser focused under the center of the poly gate. The sample was biased at 100 Vds and 0 Vgs. B: Following the approximately 27 mA transient just as the laser focal area entered the epilayer region, the SMUs recorded a sudden jump in drain current to the 21 mA limit.

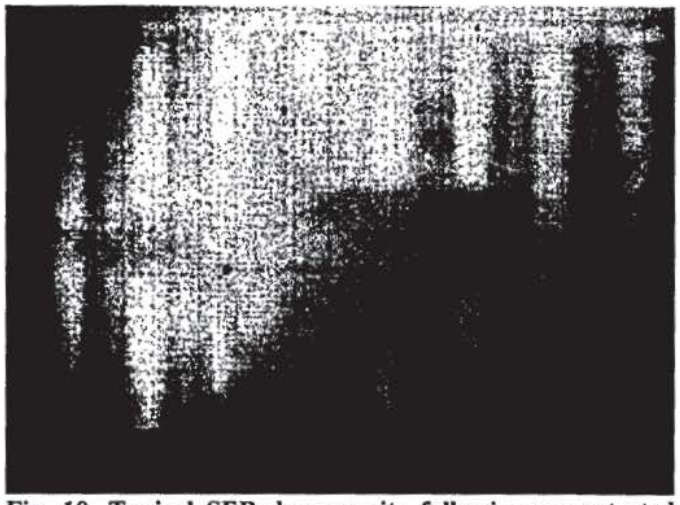

Fig. 10. Typical SEB damage site following unprotected mode TPA laser testing.

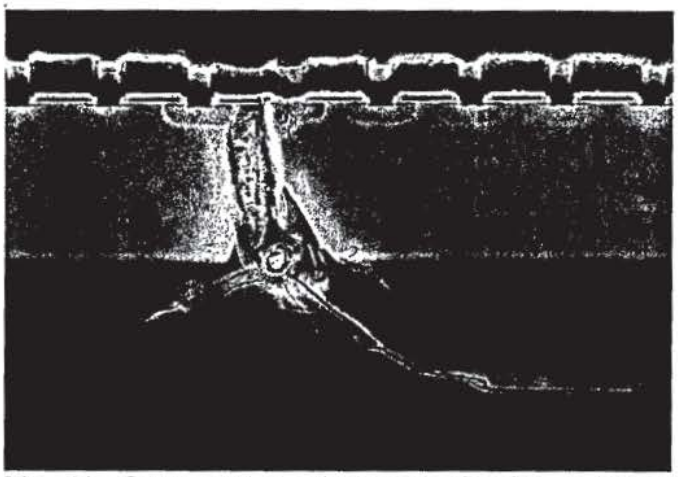

Fig. 11. Cross section micrograph showing a typical burnout site due to laser ablation (TPA).

REFERENCES

[1] A. Haran, J. Barak, D. David, N. Refaeli, B. E. Fischer, K. O. Voss, G. Du, and M. Heiss, "Mapping of Single Event Burnout in Power MOSFETs," *Nuclear Science, IEEE Transactions on,* vol. 54, pp. 2488-2494, 2007.

[2] A. Luu, P. Austin, F. Miller, N. Buard, T. Carriere, P. Poirot, R. Gaillard, M. Bafleur, and G. Sarrabayrouse, "Sensitive Volume and Triggering Criteria of SEB in Classic Planar VDMOS," *Nuclear Science, IEEE Transactions on,* vol. 57, pp. 1900-1907, 2010.

[3] A. Luu, F. Miller, P. Poirot, R. Gaillard, N. Buard, T. Carriere, P. Austin, M. Bafleur, and G. Sarrabayrouse, "SEB Characterization of Commercial Power MOSFETs With Backside Laser and Heavy Ions of Different Ranges," *Nuclear Science, IEEE Transactions on,* vol. 55, pp. 2166-2173, 2008.

[4] F. Miller, A. Luu, F. Prud'homme, P. Poirot, R. Gaillard, N. Buard, and T. Carriere, "Characterization of Single-Event Burnout in Power MOSFET Using Backside Laser Testing," *Nuclear Science, IEEE Transactions on,* vol. 53, pp. 3145-3152, 2006.

[5] O. Musseau, A. Torres, A. B. Campbell, A. R. Knudson, S. Buchner, B. Fischer, M. Schlogl, and P. Briand, "Medium-energy heavy-ion single-event-burnout imaging of power MOSFETs," *Nuclear Science, IEEE Transactions on,* vol. 46, pp. 1415-1420, 1999.

To be presented by Sandra Liu at the International Electrical and Electronics Engineering (IEEE) Nuclear and Space Radiation Effects Conference (NSREC), July 26, 2011, Las Vegas, NV., and published on nepp.nasa.gov and radhome.gsfc.nasa.gov.

[6] L. Scheick and L. Selva, "Sensitivity to LET and Test Conditions for SEE Testing of Power MOSFETs," in *2009 IEEE Radiation Effects Data Workshop*, 2009, pp. 82-93.

[7] D. Peyre, C. Binois, R. Mangeret, F. Bezerra, and R. Ecoffet, "Fluence effect on SEE response of power MOSFET," presented at the QCA RADECS Day Conf., Villigen, Switzerland, Jan. 2009.

[8] D. McMorrow, W. T. Lotshaw, J. S. Melinger, S. P. Buchner, and R. L. Pease, "Subbandgap Laser-Induced Single Event Effects: Carrier Generation via Two-Photon Absorption," *Nuclear Science, IEEE Transactions on*, vol. 49, pp. 3002-3008, 2002.

[9] J. H. Hohl and G. H. Johnnson, "Features of the triggering mechanism for single event burnout of power MOSFETs," *Nuclear Science, IEEE Transactions on*, vol. 36, pp. 2260-2266, 1989.

[10] S. Liu, J. L. Titus, and M. Boden, "Effect of Buffer Layer on Single-Event Burnout of Power DMOSFETs," *Nuclear Science, IEEE Transactions on*, vol. 54, pp. 2554-2560, 2007.

To be presented by Sandra Liu at the International Electrical and Electronics Engineering (IEEE) Nuclear and Space Radiation Effects Conference (NSREC), July 26, 2011, Las Vegas, NV., and published on nepp.nasa.gov and radhome.gsfc.nasa.gov.